Er site in Er+Au-implanted SiO$_2$: effect of annealing in reducing atmosphere

C. Maurizio[*,a], G. Perotto[b], G. Mattei[b], E. Trave[c], P. Mazzoldi[b]

[a]*INFM-CNR, OGG-European Synchrotron Radiation Facility, GILDA-CRG B.P. 220, F-38043 Grenoble, France*
[b]*Dipartimento di Fisica, Università di Padova, Via Marzolo 8, 35131 Padova, Italy*
[c]*Dipartimento di Chimica Fisica, Università Ca' Foscari, Dorsoduro 2137, 30123 Venezia, Italy*

Abstract

The Er site in Er+Au-implanted silica has been investigated by x-ray absorption spectroscopy, in particular after annealing in reducing atmosphere (H$_2$(4%):N$_2$(95%)) at temperature ranging from 100 to 800 °C. The EXAFS analysis shows that Er ions are surrounded by a first shell of O atoms, while the absence of signal from further coordination shell indicates a disordered site. The Er-O distance is lower than that of the Er$_2$O$_3$; it is suggested that the annealing in reducing atmosphere leads to a significant reduction of the first shell coordination number. Correspondingly, in the XANES region of the spectrum, it is observed a decrease in the white line intensity for annealing temperature higher than 400 °C; similar annealing treatments in inert atmosphere did not result in significant changes of the near-edge region of the x-ray absorption spectrum. These results enlighten that the annealing procedure, normally used to tailor the size distribution of the metal clusters present in the matrix and/or to modify the matrix structure, can also have an effect on the site of the Er ions, and possibly on the rare-earth optical properties.

Key words: Ion implantation, x-ray absorption spectroscopy, EXAFS, XANES, rare-earth photoluminescence, Er and metal-doped glasses

---

[*]Corresponding author
  Email address: `maurizio@esrf.fr` (C. Maurizio)

1. Introduction

Er site in silicon and silica-based matrices has been the subject of much research work, because of the interest in optimizing the Er 1.5 μm photoluminescence in view of possible applications of these materials as efficient light emitters for optoelectronics [1, 2, 3, 4, 5]. To overcome the intrinsically small cross section of the PL emission, the co-doping with Si [6, 7, 8, 9, 10] or few atoms metal aggregates [11, 12, 13, 14] has been demonstrated successful: these nano or sub-nano structures, acting as sensitizers for the Er ions, allow a broadband increase of the Er photoluminescence emission at 1.5 μm. Many different factors determine the photoluminescence emission of these composite systems: besides the site of the Er ions [3, 15, 16], the size distribution and density of the sensitizers [11] has to be finely tuned to optimize the optical properties [11, 13, 17]. To this respect, the use of Au-based structure is particularly interesting: in fact, due to the low reactivity of Au with O atoms of the matrix, specific annealing treatments at relatively low temperature can be efficiently employed to control the very early stage of the Au clusterization and finally optimize the optical emission of these systems [11, 17]. Nevertheless, these annealing processes can also have an effect on the Er site, that can turn out into a modification of the emission efficiency of the material.

In this paper, we have investigated by the x-ray absorption spectroscopy at Er L_3-edge (EXAFS, Extended X-ray Absorption Fine Structure, and XANES, X-ray Absorption Near-Edge Structure) the Er site in Er+Au sequentially implanted amorphous SiO_2, in particular after annealing in reducing atmosphere ($H_2(5\%):N_2(95\%)$) at different temperatures in the range 100-800 °C. A modification of the Er site upon annealing at temperature higher than 400 °C has been evidenced as well as a corresponding decrease of the white line intensity in the near-edge region of the x-ray absorption spectrum; the comparison with similar treatments in inert atmosphere, that do not seem to modify significantly the Er site structure or the electronic configuration, indicates that the observed changes are due to a chemical effect of the annealing atmosphere.

2. Experimental and data analysis

Pure silica slides were doped with Er and Au ions by sequential ion implantation: to extend the implanted region and to obtain an almost flat

concentration depth profile, a multiple energy implantation sequence was adopted. First, Er ions were implanted at three different energies (50, 100, 190 keV), with total fluence of 7×10^{14} Er^{+}/cm^{2}. The Er-implanted slides were then heated for 1 h in N_2 atmosphere at T=900°C to activate the luminescence of the Er ions. Then, a sequence of Au implantations at three different energies (60, 110, 190 keV) was performed with a total fluence of 7×10^{15} Au^{+}/cm^{2}. The implantation conditions of Au ions were chosen to have a maximum overlap of the Au and Er depth profiles [18]. The co-doped silica slides were then heated at different temperatures up to T = 800 °C for 1 h in reducing (5% H_2:95% N_2) or neutral (N_2) atmosphere. The sample labels indicate the heating treatment: i.e. the sample N600 was annealed in neutral atmosphere at T=600 °C whereas the sample H100 in reducing atmosphere at T=100 °C.

The EXAFS experiment was performed at the Italian beamline GILDA [19] of the European Synchrotron Radiation Facility (Grenoble-France) at the Er L_3-edge. Two series of measurements were performed: in the first one the monochromator was equipped with a couple of (311) Si crystals and in the second with (111) Si crystals. The energy resolution is pretty different in the two cases ($\approx$0.2 eV and 1.2 eV, respectively); nevertheless, the features of the x-ray absorption spectrum discussed in the following, including the white line, are much broader than the worse energy resolution, so that the comparison of spectra measured with different monochromating crystals is anyway meaningful. In both cases, the harmonic rejection was achieved by a couple of Pd-coated mirrors, working at an incidence angle of 3 mrad. Due to low Er concentration, the x-ray absorption spectra were measured in fluorescence mode with a 13-element high-purity Ge detector; the experimental geometry was properly optimized to minimize the elastic scattered radiation impinging onto the detector [20]. The EXAFS spectra of a Er_2O_3 and ErF_3 crystalline powders were also measured in transmission mode as standard references. The analysis of the EXAFS spectra was performed by the FEFF8-FEFFIT 2.98 package [21, 22]. The value of the S_0^2 parameter in the standard EXAFS formula, mainly independent from the Er surrounding atoms [23], was determined by the analysis of the ErF_3 spectrum, that is a system model since the atoms in the first shell are all located at the same coordination distance (within 0.02 Å). The Er-O backscattering phase and amplitude were calculated from a Er_2O_3 cluster, providing also to extend the calculation for different interatomic distances down to R_{Er-O} = 2.15 Å. The k^2-weighted first shell EXAFS signal was selected by a Fourier filter, then

3

fitted by a multiparameter single scattering fit into the R-space (the fitting procedure in k-space led to the same results). To reduce the number of the fitting parameters, the value of the edge energy was kept the same for all of the spectra: this procedure did not alter significantly the fit results. Moreover, since the Debye-Waller (DW) factors of the spectra for the samples annealed in the temperature range 100-400 °C were similar within the error bars, the results reported hereafter are obtained by considering the same DW for all of these spectra.

3. Results and discussion

In Figure 1 the EXAFS spectra of all the samples are shown and compared to the spectra of Er_2O_3 and ErF_3 crystalline powders. All the spectra from the samples exhibit one main oscillation, dumped at high k values, that is typical for a light backscatterer in the first atomic shell of the Er site. This signal is all located in the 1-2.5 Å region of the Fourier transform moduli reported in Figure 2(a). The quantitative analysis, whose results are shown in Table 1, indicates that for all the samples the first shell is composed of O atoms, at a distance that is shorter than that found in the crystalline Er_2O_3 oxide. The fits are superimposed to the experimental data in Figure 2(a) and (b) in R- and k-space, respectively. Signal from further coordination shell was not detectable, indicating that the Er site is strongly disordered. Moreover, since no Er-Er coordination were detected, we conclude that the most part of the Er ions are dispersed into the matrix and oxidized.
These results are well comparable with those obtained in other Er implanted Si and SiO_2-based materials [3, 2, 5], where Er ions surrounded by 5-7 atoms at a distance of about 2.21–2.24 Å are observed. It has to be noted that Er site in Er-implanted SiO_2-based systems can also exhibit a different site, characterized by a low coordination number (of about 2–3) and a short coordination distance (of about 2.05–2.10 Å) [3, 5]: this case usually occurs at low Er concentration, i.e. when the low radiation damage associated with the Er implantation does not strongly favor the formation of Er-O bonds with respect to Si-O ones [3]; in the present case the Er total fluence is low, but after the Er implantation a sequence of Au implants have been performed: the radiation damage associated could likely favored the formation of Er sites with higher coordination number (and longer coordination distance), more similar to the Er site in the corresponding oxide [3].
About the effect of the annealing in reducing atmosphere, the EXAFS re-

sults indicate that the coordination number, that is about 7 after annealing at T ≤ 200 °C, progressively decreases with the increase of the annealing temperature, down to about 5 upon annealing at 800 °C. The Debye Waller factor decreases above T ≥ 600 °C, indicating a progressive ordering of the Er site. At this point, it has to be remarked that in the EXAFS analysis the first shell coordination number and Debye-Waller factor are two strongly correlated variables in the fit, so that the increase of one of the two could be at least partially compensated by the increase of the other one. To better investigate this point, in Figure 3 we compare the first shell-filtered signal (in k-space) for the sample N800 with two different fits: the first one (a) is the same as in Figure 2(b), i.e. N and σ^2 were both fitting variables, while the second (b) is obtained by fixing σ^2 at the value estimated for the samples annealed at T ≤ 400 deg (σ^2= 0.021 Å^2): it is clear that, while the frequency of the EXAFS oscillation is pretty well reproduced by both, the fit 'b' does not reasonably reproduce the amplitude of the oscillations, since the experimental signal in the high-k region is higher than the theoretical curve that consider a high DW factor. Quantitatively, the R-factor [24] and the reduced χ square is six times higher in case 'b' with respect to case 'a'. This indicates that actually the decrease of the DW factor observed for the sample N800 is effective, i.e. the first shell signal is in agreement with an ordered and low-coordinated site and cannot be properly simulated with an O shell with the same structural disorder as for the sample H100.

To fully investigate any possible effect of the annealing atmosphere on the Er site, further analysis are needed, in particular on two complete series of samples annealed at different temperatures in the two atmospheres. Nevertheless, from our data a preliminary comparison can be made between the Er average site in two samples (N550 and H600) that are annealed in a temperature range where the silica matrix begins to re-arrange and recover from the damage produced during the Au implantation process. The results (see Table 1) suggest a chemical effect induced by the annealing atmosphere on the Er site, in the sense that the Er site seems to remain more disordered upon annealing in inert atmosphere (the DW factor is higher) than in reducing one and that, correspondingly, the coordination number is slightly higher and the coordination distance longer upon N$_2$-annealing.

Some interesting information on the chemical effect of the annealing atmosphere can be obtained by comparing the XANES spectra of Er+Au-implanted silica measured after annealing in reducing or inert atmosphere at different temperatures. In Figure 4(a) the XANES spectra recorded be-

fore and after heating in neutral atmosphere at different temperatures are reported, and compared to the spectra of Er_2O_3 and ErF_3. The photoelectric absorption edge from the $2p_{3/2}$ state (L_3-edge) is characterized in all cases by a sharp absorption (whiteline), due to the electronic transition to the empty $5d$ states. In the inset of the same Figure a zoom of the white line maximum region is shown: it is clear that the white line intensity remain stable. In Figure 4(b) the XANES spectra after annealing in reducing atmosphere are shown: while the white line intensity is the same upon annealing in reducing atmosphere up to 400 °C and after annealing in neutral atmosphere at 550 °C a significant and progressive decrease of the white line intensity occurs after annealing at T $\geq$ 600 °C in reducing atmosphere: after 800 °C annealing in reducing atmosphere the white line is about the 80% of its original height. To this respect it has to be noted that the white line intensity depends on several factors, as the occupancy of the $5d$ state as well as the degree of disorder (i.e. the width of the first shell interatomic distance distribution). In particular, a stronger white line is expected for a stronger ionic character and more ordered sites. To this respect, we note that the white line is stronger for the ErF_3 than for Er_2O_3 (where two sites for Er ions are present) and that the intensity of the white line for all the samples is in between the two (see Figure 4). It has to be noted that we did not observe any energy shift of the Er edge position with respect to the Er_2O_3 or ErF_3, suggesting the absence of major changes in the 3+ average oxidation state; moreover, in the present case the white line intensity decreases for Er sites less disordered (low DW). Our results suggest that the annealing in reducing atmosphere promotes a partial progressive filling of the $5d$-states of the Er ions. The decrease of the white line intensity seems to be related to the electronic reconfiguration induced by the decrease of the first shell coordination number; further analyses are in progress to better investigate this point, also to evidence a possible effect on the optical properties of the Er ions.

4. Conclusions

We have investigated by x-ray absorption spectroscopy the Er site in Er+Au sequentially implanted silica, after annealing in reducing atmosphere. The EXAFS analysis indicates a disordered site, where only a first Er-O distance is present. The Er-O distance and coordination number for annealing at T≤400°C are typical of Er-implanted silica-based materials. The annealing at higher temperature induces a progressive decreasing of the coordination

6

number; correspondingly, the XANES spectra suggest a progressive filling of the 5d electronic states. It is shown that the same annealing in neutral atmosphere did not induce similar changes, indicating a chemical effect of the annealing atmosphere on the Er site. These results show that the thermal treatments on Er- and/or Er+metal-doped silica-based systems, that are normally performed to modify the matrix structure or the metal aggregation state can have an effect on the Er site as well, and so possibly on the rare-earth optical properties.

References

[1] C. Piamonteze, A. C. Iñiguez, L. R. Tessler, M. C. Martins Alves, H. Tolentino, Phys. Rev. Lett. 81 (1998) 4652.

[2] F. D'Acapito, S. Mobilio, A. Scalese, S. amd Terrasi, G. Franzò, F. Priolo, Phys. Rev. B 69 (2004) 153310.

[3] C. Maurizio, F. Iacona, F. D'Acapito, G. Franzò, F. Priolo, Phys. Rev. B 74 (2006) 205428.

[4] C. Maurizio, F. D'Acapito, F. priolo, G. Franzo, F. Iacona, E. Borsella, S. Padovani, P. Mazzoldi, Optical Materials 27 (2005) 900.

[5] M. A. Marcus, D. Jacobson, A. Vredenberg, G. Lamble, J. Non-Cryst. Solids 195 (1996) 232–238.

[6] A. J. Kenyon, P. F. Trwoga, M. Federighi, C. W. Pitt, J. Phys.: Condens. Matter 6 (1994) L319.

[7] M. Fujii, M. Yoshida, Y. Kanzawa, S. Hayashi, K. Yamamoto, Appl. Phys. Lett. 71 (1997) 1198.

[8] G. Franzò, S. Boninelli, D. Pacifici, F. Priolo, F. Iacona, C. Bongiorno, Appl. Phys. Lett.

[9] P. G. Kik, M. L. Brongersma, A. Polman, Appl. Phys. Lett. 76 (2000) 2325.

[10] F. Enrichi, G. Mattei, C. Sada, E. Trave, D. Pacifici, G. Franzo, F. Priolo, F. Iacona, M. Prassas, M. Falconieri, E. Borsella, Evidence of energy transfer in an aluminosilicate glass codoped with si nanoaggregates and

er[sup 3+] ions, Journal of Applied Physics 96 (7) (2004) 3925–3932. doi:10.1063/1.1776637.
URL http://link.aip.org/link/?JAP/96/3925/1

[11] E. Trave, G. Mattei, P. Mazzoldi, G. Pellegrini, C. Scian, C. Maurizio, G. Battaglin, Sub-nanometric metallic au clusters as efficient er[sup 3+] sensitizers in silica, Applied Physics Letters 89 (15) (2006) 151121. doi:10.1063/1.2266229.
URL http://link.aip.org/link/?APL/89/151121/1

[12] C. Strohhofer, A. Polman, Silver as a sensitizer for erbium, Applied Physics Letters 81 (8) (2002) 1414–1416. doi:10.1063/1.1499509.
URL http://link.aip.org/link/?APL/81/1414/1

[13] A. Martucci, M. D. Nuntis, A. Ribaudo, M. Guglielmi, S. Padovani, F. Enrichi, G. Mattei, P. Mazzoldi, C. Sada, E. Trave, G. Battaglin, F. Gonella, E. Borsella, M. Falconieri, M. Patrini, J. Fick, Appl. Phys. A 80 (2004) 557.

[14] M. Fukushima, N. Managaki, M. Fujii, H. Yanagi, S. Hayashi, Enhancement of 1.54-mu m emission from er-doped sol-gel sio[sub 2] films by au nanoparticles doping, Journal of Applied Physics 98 (2) (2005) 024316. doi:10.1063/1.1990257.
URL http://link.aip.org/link/?JAP/98/024316/1

[15] A. Terrasi, G. Franzò, S. Coffa, F. Priolo, F. D'Acapito, S. Mobilio, Appl. Phys. Lett. 70 (1997) 1712.

[16] D. L. Adler, D. C. Jacobson, D. J. Eaglesham, M. A. Marcus, J. L. Benton, J. M. Poate, P. H. Citrin, Appl. Phys. Lett. 61 (1992) 2181.

[17] C. Maurizio, *et al.*, submitted.

[18] J. P. Biersack, L. Haggmark, Nucl. Instr. Methods 174 (1980) 257.

[19] F. e. a. D'Acapito, ESRF Newsletter 30 (1998) 42.

[20] C. Maurizio, M. Rovezzi, F. Bardelli, H. G. Pais, F. D'Acapito, Setup for optimized grazing incidence x-ray absorption experiments on thin films on substrates, Review of Scientific Instruments 80 (6) (2009) 063904–6. doi:10.1063/1.3155791.
URL http://link.aip.org/link/?RSI/80/063904/1

8

[21] A. Ankudinov, B. Ravel, J. Rehr, M. Newville, FEFFFIT manual within the FEFF project, University of Washington, Seattle, USA, 1992-1999.

[22] A. L. Ankudinov, J. J. Rehr, S. D. Conradson, Real-space multiple-scattering calculation and interpretation of x-ray-absorption near-edge structure, Physical Review B 58 (12) (1998) 7565–7576. doi:10.1103/PhysRevB.58.7565.
URL http://link.aps.org/doi/10.1103/PhysRevB.58.7565

[23] J. J. Rehr, R. C. Albers, Rev. Mod. Phys. 72 (2000) 621.

[24] Error reporting recommendations adopted by the ixs standards and criteria committee (http://ixs.csrri.iit.edu/) (2000).

[25] Y. A. Malinovskii, O. S. Bondareva, Kristall. 36 (1991) 1558.

[26] K. Kraemer, H. Romstedt, H. U. Guedel, P. Fischer, A. Murasik, M. T. Fernandez-Diaz, Europ. J Sol. State In. Chem. 36 (1996) 273.

Table 1: EXAFS results of the first shell of O atoms around Er: N is the coordination number, R the Er-O distance and σ^2 the DW factor. The results for the first shell of the crystalline powders Er_2O_3 (Er-O coordination) and ErF_3 (Er-F coordination) are shown for comparison: the corresponding crystallographic values are reported in parenthesis [25, 26].

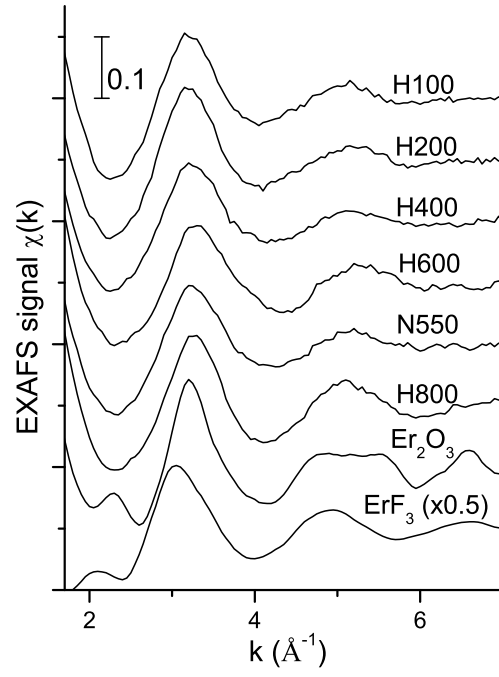| sample name	N	R (Å)	σ^2 ($\times 10^{-3}$Å^2)
H100	6.8±0.7	2.23±0.02	21±3
H200	7.0±0.7	2.24±0.02	21±3
H400	6.1±0.6	2.20±0.02	21±3
H600	4.7±0.8	2.17±0.02	10±4
H800	5.0±0.7	2.22±0.02	6±3
N550	6.2±0.8	2.22±0.02	22±5
Er_2O_3	6	2.25±0.01	7±1
	(3;1;1)	(2.27;2.24;2.31)	–
ErF_3	8 F	2.28±0.01	9±1
	(8 F)	(2.28–2.30)	–

Figure 1: EXAFS spectra recorded at Er L_3-edge of the Er+Au implanted silica samples, after different heating treatments, compared to the spectra of Er_2O_3 and ErF_3 crystalline powders.
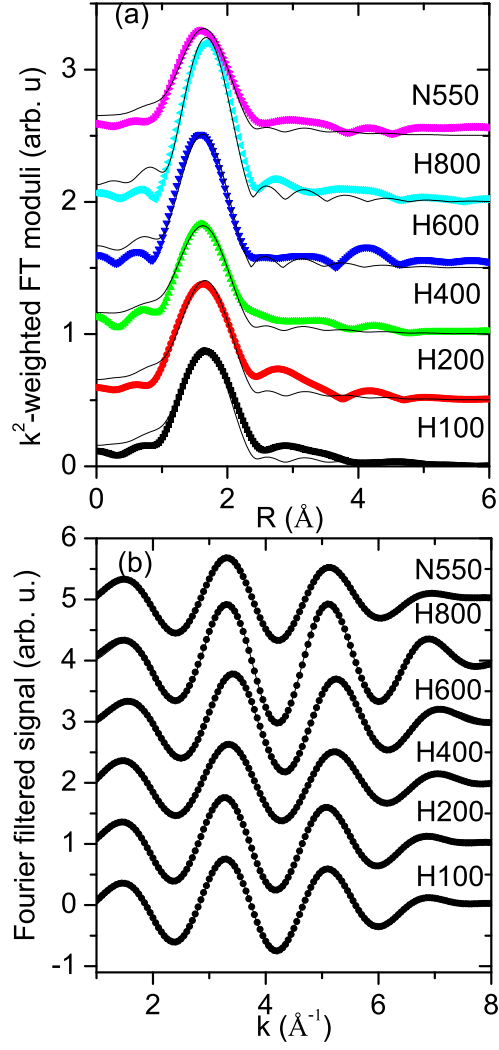
Figure 2: (a) k^2-weighted Fourier transform moduli (markers, in the range $k = 1.8$–7 Å^{-1}) and relative first shell fits (solid line). (b) Fourier filtered signals (markers, in the range $R = 1.2$–2.3 Å) and relative first shell fits (solid line) in the k-space.
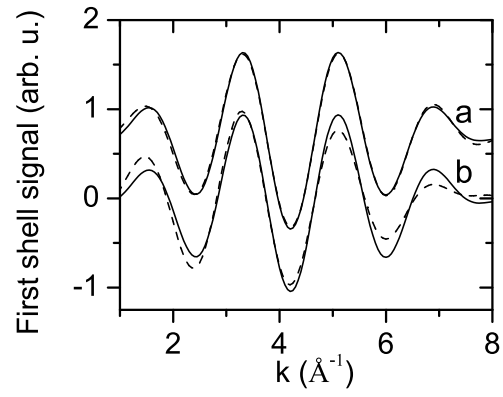
Figure 3: EXAFS analysis for the N800 sample: the experimental first shell signal (solid line) is compared to two different fits (dashed lines): in 'a' the fit considered no constraint on N and σ^2 parameters; in 'b' the fitting procedure considered a fix DW factor ($\sigma^2 = 21 \times 10^{-3}$ Å^2)
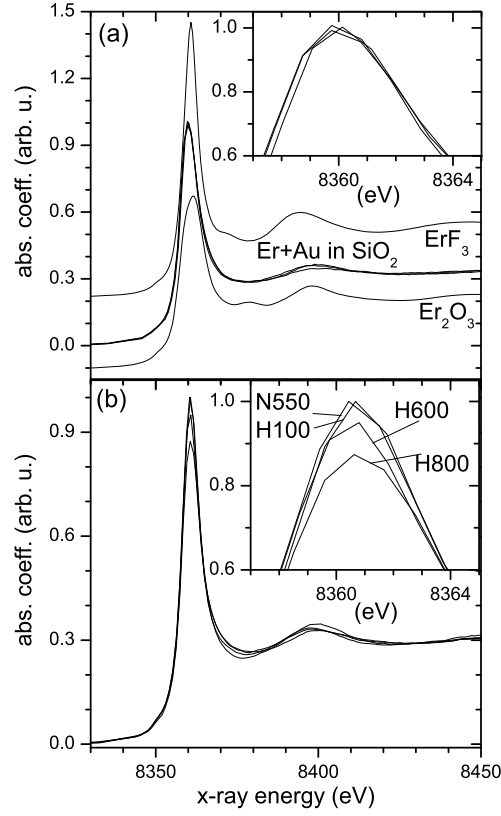
.

Figure 4: (a) XANES spectra of Er+Au implanted SiO$_2$, before and after annealing in N$_2$ atmosphere at 400 °C and 800 °C, compared to the spectra of Er$_2$O$_3$ and ErF$_3$ crystalline compounds; in the inset the white line peak region for the implanted samples is zoomed. (b) XANES spectra of Er+Au implanted SiO$_2$ annealed in H$_2$ atmosphere at 100 °C, 600 °C and 800 °C are compared to the spectrum of the sample annealed at 550 °C in N$_2$; in the inset the white line peak region is zoomed. The spectra of the samples H200 and H400, not reported, are identical to H100.